ChemComm

COMMUNICATION

View Article Online
View Journal | View Issue

Cite this: *Chem. Commun.*, 2014, 50, 14983

Received 27th September 2014,
Accepted 10th October 2014

DOI: 10.1039/c4cc07628a

www.rsc.org/chemcomm

A monomeric photosensitizer for targeted cancer therapy†

Ruizheng Liang,[a] Lina Ma,[b] Lele Zhang,[b] Chunyang Li,[a] Wendi Liu,[a] Min Wei,*[a] Dan Yan,*[b] David G. Evans[a] and Xue Duan[a]

A targeted photosensitizer used in photodynamic therapy (PDT) was fabricated by incorporation of zinc phthalocyanine (ZnPc) and folic acid (FA) into polyvinylpyrrolidone (PVP) micelles, which exhibits excellent anticancer performance revealed by both *in vitro* studies and *in vivo* tests.

Photodynamic therapy (PDT), which is a promising therapeutic methodology for cancer treatment, has attracted considerable interest owing to its facile and non-invasive modality with minimal side effects. The principle of PDT involves the injection of a photosensitizer followed by red or near-IR light irradiation to generate singlet oxygen that induces an effective destruction of tumor tissues.[1] PDT has shown significant development with the key contribution of photosensitizers, which is regarded as the research focus of this area.[2] An ideal photosensitizer should possess the following properties: (1) a monodisperse photosensitizer is the most favorable state, owing to its powerful capability to generate singlet oxygen; (2) the photosensitizer can be activated in near-IR light to allow a remarkable tissue penetration to deep-seated cancer cells;[3] (3) a targeted ability toward tumor is highly desirable, in terms of inhibiting side effects to normal cells.[4] However, it is a difficult conundrum to obtain a photosensitizer that reaches the three requirements simultaneously.

To satisfy the above mentioned prerequisites, many types of drug delivery vehicles, such as polymeric micelles, conjugated polymer nanoparticles, inorganic nanoparticles, have been extensively explored to fabricate a stable dispersion of photosensitizer drugs in aqueous systems.[5,6] Although nanoparticle-based systems can achieve enhanced permeability and a retention (EPR) effect that tend to accumulate in tumor tissue more than normal tissues and realize passive targeting of the tumor,[7] active targeting of nanoparticles can be further obtained through the conjugation of biological ligands (*e.g.*, antibodies, peptides, carbohydrates, and folic acid) with an affinity for a specific surface receptor expressed by cancer cells.[6a,8] Therefore, a combination of a photosensitizer, a biological ligand and a delivery vehicle to realize the unified delivery, targeting and therapy is believed as the key issue in the PDT field. In spite of great progress, how to fabricate a composite photosensitizer with monomeric species, near-IR light response, targeted anticancer behavior, high biocompatibility and stability is still a tremendous challenge in this area.

Herein, we report the preparation of a multifunctional delivery vehicle, which involves a photosensitizer (zinc phthalocyanine, ZnPc) and a targeting agent (folic acid, FA) encapsulated within a water-soluble polyvinylpyrrolidone (PVP) micelle (denoted ZnPc–FA/PVP). The encapsulated FA achieves a targeted cancer therapy owing to its over-expression toward cancer cells.[9] UV-vis spectroscopy confirms that the ZnPc molecules are accommodated within polymer micelles in the monomeric state, resulting in a largely-enhanced efficiency of singlet oxygen production. *In vitro* studies performed with HepG2 cell and *in vivo* tests over mice reveal a satisfactory PDT effectiveness of the ZnPc–FA/PVP photosensitizer. The simultaneous monomeric dispersion, near-IR light activity, *in vivo* imaging and targeted therapy are the most distinct features of the composite photosensitizer reported in this work.

The encapsulation of ZnPc within PVP was firstly studied by the preparation of steady colloidal suspension *via* tuning the ratio of ZnPc/PVP (see details in the ESI†). Fig. 1A shows the UV absorption spectra of several colloidal suspensions with the same ZnPc concentration whilst various ZnPc/PVP ratios. An absorption maximum at 635 nm is observed for the ZnPc aqueous solution, corresponding to its dimer or multimer (H-type aggregates) in high polarity media.[10] For the ZnPc in 60% ethanol solution, the absorption maximum moves to 675 nm, indicating the collapse of H-type aggregation and the presence of a monomeric state in low polarity media. In the case of the ZnPc(5.88%)/PVP aqueous suspension, only a strong absorption at 682 nm is observed, suggesting that PVP micelles provide a low polarity microenvironment for the existence of monomeric ZnPc. We also investigated

[a] *State Key Laboratory of Chemical Resource Engineering, Beijing University of Chemical Technology, Beijing 100029, P. R. China. E-mail: weimin@mail.buct.edu.cn; Fax: +86-10-64425385; Tel: +86-10-64412131*

[b] *Military Institute of Chinese Materia Medica, 302th Military Hospital of China, Beijing 100039, P. R. China. E-mail: yd277@126.com*

† Electronic supplementary information (ESI) available. See DOI: 10.1039/c4cc07628a

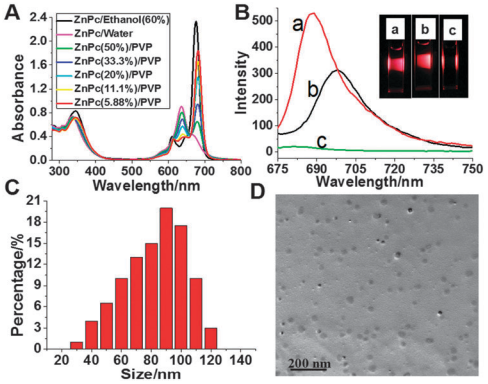

Fig. 1 (A) The UV-vis absorption spectra of: pristine ZnPc in aqueous solution, in 60% ethanol and ZnPc(*x*%)/PVP with *x* ranging in 5.88–50%. (B) The photoluminescence spectra of (a) ZnPc in 60% ethanol, (b) ZnPc(5.88%)/PVP suspension, (c) ZnPc solution. The inset shows their photographs: (a) ZnPc in 60% ethanol solution, (b) ZnPc(5.88%)/PVP suspension, (c) ZnPc solution. (C) Particle size distribution and (D) the TEM image of ZnPc(5.88%)–FA/PVP.

the employment of several other polymers (*e.g.*, polyacrylamide (PAM), poly(ethyleneglycol) (PEG), polyacrylic acid (PAA), polyvinyl alcohol (PVA), poly(sodium-*p*-styrenesulfonate) (PSS)) for the loading of ZnPc, and found that only PVP can achieve the monomeric state of ZnPc (Fig. S1, ESI†). A hydrogen bond interaction between ZnPc and PVP may contribute to the disaggregation of ZnPc, which was confirmed by FT-IR spectra (Fig. S2A, ESI†). The carbonyl stretching band of pristine PVP (1655 cm^{-1}) shifts to low frequency (1645 cm^{-1}) after the combination with ZnPc, suggesting the formation of a hydrogen bond between PVP and ZnPc. Similar phenomena have also been reported previously in the PVP-containing micelle systems.[11] Fig. 1B displays the photoluminescence (PL) spectra of 50 μg mL^{-1} of pristine ZnPc in aqueous solution, in 60% ethanol solution and ZnPc(5.88%)/PVP solution, respectively. Compared with the former two samples, ZnPc(5.88%)/PVP shows a red-shift emission peak at 699 nm with a moderate intensity, implying the potential application in the near-IR fluorescence imaging. The photographs in Fig. 1B further give a visual result: both the ZnPc ethanol solution (Fig. 1B-a) and ZnPc(5.88%)/PVP solution (Fig. 1B-b) show much stronger red emission in contrast to the ZnPc aqueous solution (Fig. 1B-c). In the next step, ZnPc(5.88%)–FA/PVP was further prepared by encapsulation of ZnPc and FA into PVP micelles with the desired ratio (Fig. S3A, ESI†). Both the dialysis test and FT-IR spectra indicate the incorporation of FA and ZnPc in the micelle (Fig. S2B and S3B, ESI†). The equivalent hydrodynamic diameter of ZnPc(5.88%)–FA/PVP in aqueous solution was determined to be ~90 nm (Fig. 1C) by the dynamic light scattering (DLS) measurements. The Zeta potential values of ZnPc(5.88%)/PVP and ZnPc(5.88%)–FA/PVP are −10.8 and −29.1 mV, respectively (Fig. S4, ESI†), facilitating their stable dispersion in aqueous solution. The TEM image (Fig. 1D) also shows that the sample of ZnPc(5.88%)–FA/PVP possesses a uniform morphology of spherical vesicles with a diameter ranging from 20 to 60 nm, which is somewhat lower than the DLS measurements.

The generation of singlet oxygen by ZnPc(*x*%)/PVP was detected chemically using the disodium salt of 9,10-anthracenedipropionic acid (ADPA) as a detector.[4] Fig. S5 (ESI†) displays the decrease in absorbance at 378 nm by ADPA with the presence of various samples as a function of irradiation time under 650 nm. For the ADPA solution, no any change in its absorbance is observed under light irradiation (Fig. S5A, ESI†). The addition of pristine ZnPc into ADPA solution accelerates this process (Fig. S5B, ESI†), indicating that ADPA reacts with the singlet oxygen generated by ZnPc. In the cases of the presence of ZnPc(*x*%)/PVP materials, a sharp decrease in absorbance is observed (Fig. S5C–G, ESI†). The results show that the production of singlet oxygen enhances gradually along with the decrease of ZnPc loading from 50% to 5.88%, and the sample of ZnPc(5.88%)/PVP exhibits the strongest capability to produce singlet oxygen (Fig. S5H, ESI†). In addition, Fig. S6 (ESI†) gives the photostability of the ZnPc–PVP composite in comparison with pristine ZnPc. After a continuous irradiation under 650 nm for 30 min, the absorbance of pristine ZnPc at 682 nm decreases 29.6% while only 7.1% and 10.9% loss are observed for ZnPc(5.88%)/PVP and ZnPc(11.1%)/PVP, respectively. This indicates that the ZnPc/PVP system possesses a better resistance against photobleaching than pristine ZnPc.

The PDT performance of the ZnPc(5.88%)–FA/PVP composite photosensitizer was further studied by *in vitro* tests performed with HepG2 cells. The impact of FA content was firstly investigated. The HepG2 cells were incubated in the ZnPc(5.88%)–FA/PVP suspension (equivalent ZnPc 10 μg mL^{-1}) with various FA contents for 24 h. Based on the fluorescence intensity of HepG2 lysate samples (Fig. S7, ESI†), FA obviously facilitates the cellular uptake of the photosensitizer and the best mass ratio of ZnPc to FA is 1 : 4. Fig. S8 (ESI†) displays the PDT effectiveness of ZnPc(*x*%)–FA/PVP (ZnPc : FA = 1 : 4) photosensitizers with various concentrations. A significant PDT effect occurs and enhances gradually along with the increase of dosage from 0.5 to 10 μg mL^{-1}, and no obvious improvement can be obtained with further increase (from 10 to 50 μg mL^{-1}). At the same photosensitizer concentration, the sample of ZnPc(5.88%)–FA/PVP displays superior PDT performance, in agreement with the spectral characterization discussed above. The best PDT behavior was demonstrated for ZnPc(5.88%)–FA/PVP (dosage:10 μg mL^{-1}), resulting in a cell death of 94.3%.

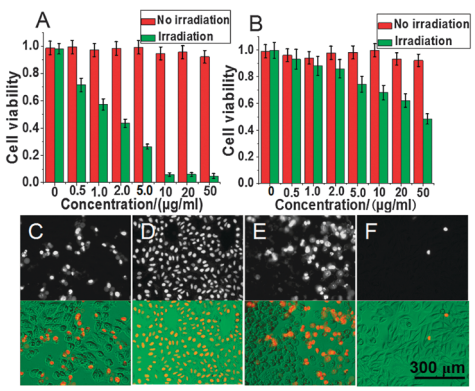

Fig. 2 PDT performances of (A) ZnPc(5.88%)–FA/PVP and (B) ZnPc(5.88%)/PVP with the concentration from 0 to 50 μg mL^{-1}. Fluorescence microscopy and merged images of HepG2 cells treated with various photosensitizers with irradiation (10 μg mL^{-1}, 24 h incubation): (C) ZnPc, (D) ZnPc(5.88%)–FA/PVP, (E) ZnPc(5.88%)/PVP, (F) blank.

In order to shed light on the function of FA, Fig. 2A and B show the PDT performance of ZnPc(5.88%)–FA/PVP and ZnPc(5.88%)/PVP with the concentration ranging from 0 to 50 μg mL^{-1}, respectively. A minimal dark toxicity is observed for both of the two photosensitizers; while the coexistence of FA and ZnPc results in a largely-enhanced PDT behavior in contrast to the individual ZnPc, demonstrating the effectiveness of FA for specifically targeting HepG2 cells. Fig. S9 (ESI†) shows that the fluorescence intensity of ZnPc(5.88%)–FA/PVP in the cell lysate sample is much stronger than that of ZnPc(5.88%)/PVP with the photosensitizer concentration from 1 to 10 μg mL^{-1}. As a result, the ZnPc(5.88%)–FA/PVP exhibits targeted performance *via* the over-expression of FA toward HepG2 cells, accounting for its largely-enhanced cellular uptake and PDT efficacy. For comparison, the phototoxicity of ZnPc was also studied and both the PDT effect and cytotoxicity enhance gradually along with the increase of dosage (Fig. S10, ESI†). In order to visualize the phototoxicity results, the presence of dead cells after PDT was evaluated by staining with propidium iodide (PI). HepG2 cells treated with 10 μg mL^{-1} of ZnPc, ZnPc(5.88%)–FA/PVP, ZnPc(5.88%)–PVP and the blank test with and without irradiation are displayed in Fig. 2C–F and Fig. S11 (ESI†). The results reveal that the ZnPc(5.88%)–FA/PVP photosensitizer displays superior PDT effectiveness and low cytotoxicity, in accordance with the *in vitro* tests above.

In vivo PDT performance of the ZnPc(5.88%)–FA/PVP photosensitizer was further studied on male Balb/c mice from the viewpoint of practical applications. Firstly, 100 μL of ZnPc(5.88%)–FA/PVP suspension (equivalent ZnPc 50 μg) was injected intravenously into mice, and *in vivo* fluorescence imaging was recorded on a Carestream Molecular Imaging In-Vivo MS FX PRO system. As shown in Fig. 3A, the signal from tumor (at hind flank of the mouse) gradually becomes strong (0–2 h), indicating a good targeted ability of ZnPc(5.88%)–FA/PVP in the mice. In contrast, for the whole metabolic process of ZnPc(5.88%)/PVP after intravenous injection, no obvious intense fluorescence signal from the tumor at the same position can be observed. The results show that ZnPc(5.88%)–FA/PVP can be used as a good near-IR agent for *in vivo* targeting imaging. We further evaluated the *in vivo* therapeutic efficacy of ZnPc(5.88%)–FA/PVP-induced PDT cancer treatment. Four groups of HepG2 tumor-bearing mice (8 animals per group) were employed in this work. For the target group, tumors were intravenously injected with ZnPc(5.88%)–FA/PVP (dosage: 2 mg kg^{-1}) and then irradiated by a simulated sunlight source (optical filter 650 ± 5 nm) with a power density of 20 mW cm^{-2} for 30 min (fluence rate: 36 J cm^{-2}). Other control groups consist of saline injection with irradiation, ZnPc injection with irradiation, ZnPc(5.88%)/PVP injection with irradiation. The tumor size was measured using a caliper every day after treatment. It was found from Fig. 3B that the *in vivo* PDT efficiency increases by the following order: saline < ZnPc < ZnPc(5.88%)/PVP < ZnPc(5.88%)–FA/PVP. The ZnPc(5.88%)–FA/PVP photosensitizer exhibits the best *in vivo* PDT behavior. This striking contrast can be further visualized by the mice photograph after treatment of 14 days (Fig. 3C). In addition, haematoxylin and eosin (H&E) staining of tumor slices was also carried out one day after treatment for all the four groups (Fig. 3D). As expected, significant cancer cell damage was noticed in the tumor with ZnPc(5.88%)–FA/PVP injection and irradiation (Fig. 3D: d); while no obvious necrosis/apoptosis can be observed in the other three control groups (Fig. 3D: a–c). The excellent anticancer performance of ZnPc(5.88%)–FA/PVP *in vivo* makes it a promising agent in PDT area, which would guarantee its practical applications.

In summary, a targeted photosensitizer used in PDT was fabricated by incorporation of ZnPc and FA into PVP micelles. The hydrophobic microenvironment results in the dispersion of ZnPc as the monomeric state in PVP micelles, with large singlet oxygen production efficiency. *In vitro* studies performed with HepG2 cells reveal that the ZnPc(5.88%)–FA/PVP composite photosensitizer exhibits a satisfactory PDT effectiveness (equivalent 10 μg mL^{-1} ZnPc induces 94.3% cell death), good biocompatibility and low cytotoxicity. This can be attributed to the enhanced singlet oxygen production efficiency and largely-elevated cellular uptake through the over-expression of FA toward HepG2 cells. *In vivo* tests demonstrate an *in vivo* imaging and excellent PDT behavior, with an ultra-low dose of 2 mg kg^{-1} and a low optical fluence rate of 36 J cm^{-2}. The targeted photosensitizer in this work can be potentially used in the field of PDT.

This work was supported by the 973 Program (Grant No. 2014CB932102), the National Natural Science Foundation of China (NSFC), the Fundamental Research Funds for the Central Universities (ZD 1303). M. Wei and D. Yan appreciate the financial aid from the China National Funds for Distinguished/Excellent Young Scientists of the NSFC.

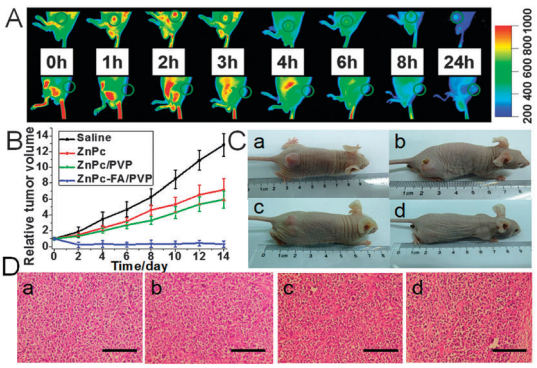

Fig. 3 (A) *In vivo* fluorescence imaging of mice after intravenous injection with 100 μL of ZnPc(5.88%)–FA/PVP (above) and ZnPc(5.88%)/PVP (below) at different time points. (B) The tumor growth curves of the four groups of mice after treatment. (C) Representative photos of mice bearing HepG2 tumors after various treatments of 14 days. (D) H&E stained tumor slices collected from the four groups after 24 h treatment (the scale bar is 300 μm).

Notes and references

1 (*a*) A. Castano, P. Mroz and M. Hamblin, *Nat. Rev. Cancer*, 2006, **6**, 535; (*b*) M. J. Sailor and J. H. Park, *Adv. Mater.*, 2012, **24**, 3779; (*c*) P. Zhang, W. Steelant, M. Kumar and M. Scholfield, *J. Am. Chem. Soc.*, 2007, **129**, 4526; (*d*) A. N. Amin, M. E. El-Khouly, N. K. Subbaiyan, M. E. Zandler, S. Fukuzumi and F. D'Souza, *Chem. Commun.*, 2012, **48**, 206.
2 K. Lang, J. Mosinger and D. M. Wagnerová, *Coord. Chem. Rev.*, 2004, **248**, 321.
3 (*a*) U. Basu, I. Khan, A. Hussain, P. Kondaiah and A. R. Chakravarty, *Angew. Chem., Int. Ed.*, 2012, **51**, 2658; (*b*) J. Shan, S. J. Budijono,

G. Hu, N. Yao, Y. Kang, Y. Ju and R. K. Prud' homme, *Adv. Funct. Mater.*, 2011, **21**, 2488; (*c*) R. B. Vegh, K. M. Solntsev, M. K. Kuimova, S. Cho, Y. Liang, B. L. W. Loo, L. M. Tolbert and A. S. Bommarius, *Chem. Commun.*, 2011, **47**, 4887.

4 G. Obaid, I. Chambrier, M. J. Cook and D. A. Russell, *Angew. Chem., Int. Ed.*, 2012, **51**, 6158.

5 (*a*) W.-D. Jang, N. Nishiyama, G.-D. Zhang, A. Harada, D.-L. Jiang, S. Kawauchi, Y. Morimoto, M. Kikuchi, H. Koyama, T. Aida and K. Kataoka, *Angew. Chem., Int. Ed.*, 2005, **44**, 419; (*b*) K. J. Son, H.-J. Yoon, J.-H. Kim, W.-D. Jang, Y. Lee and W.-G. Koh, *Angew. Chem., Int. Ed.*, 2011, **50**, 11968; (*c*) R. Liang, M. Wei, D. G. Evans and X. Duan, *Chem. Commun.*, 2014, DOI: 10.1039/C4CC03118K.

6 (*a*) M. Gary-Bobo, Y. Mir, C. Rouxel, D. Brevet, I. Basile, M. Maynadier, O. Vaillant, O. Mongin, M. Blanchard-Desce, A. Morère, M. Garcia, J.-O. Durand and L. Raehm, *Angew. Chem., Int. Ed.*, 2011, **50**, 11425; (*b*) H.-L. Tu, Y.-S. Lin, H.-Y. Lin, Y. Hung, L.-W. Lo, Y.-F. Chen and C.-Y. Mou, *Adv. Mater.*, 2009, **21**, 172; (*c*) B. Tian, C. Wang, S. Zhang, L. Feng and Z. Liu, *ACS Nano*, 2011, **5**, 7000; (*d*) C. Wang, L. Cheng, Y. Liu, X. Wang, X. Ma, Z. Deng, Y. Li and Z. Liu, *Adv. Funct. Mater.*, 2013, **23**, 3077; (*e*) M. Brasch, A. Escosura, Y. Ma, C. Uetrecht, A. J. R. Heck, T. Torres and J. J. L. M. Cornelissen, *J. Am. Chem. Soc.*, 2011, **133**, 6878.

7 H. Maeda, J. Fang, T. Inutsuka and Y. Kitamoto, *Int. Immunopharmacol.*, 2003, **3**, 319.

8 (*a*) T. Stuchinskaya, M. Moreno, M. J. Cook, D. R. Edwards and D. A. Russell, *Photochem. Photobiol. Sci.*, 2011, **10**, 822; (*b*) H. J. Hah, G. Kim, Y.-E. k. Lee, D. A. Orringer, O. Sagher, M. A. Philbert and R. Kopelman, *Macromol. Biosci.*, 2011, **11**, 90; (*c*) S.-J. Yang, F.-H. Lin, H.-M. Tsai, C.-F. Lin, H.-C. Chin, J.-M. Wong and M.-J. Shieh, *Biomaterials*, 2011, **32**, 2174.

9 (*a*) H. Zhou, P. Jiao, L. Yang, X. Li and B. Yan, *J. Am. Chem. Soc.*, 2011, **133**, 680; (*b*) B. Liang, M.-L. He, C. Chan, Y. Chen, X.-P. Li, Y. Li, D. Zheng, M. C. Lin, H.-F. Kung, X.-T. Shuai and Y. Peng, *Biomaterials*, 2009, **30**, 4014.

10 K. M. Kadish, K. M. Smith and R. Guilard, *Handbook of Porphyrin Science*, World Scientific, Singapore, 2010.

11 (*a*) L. S. Taylor and G. Zografi, *Pharm. Res.*, 1997, **14**, 1691; (*b*) K. Imamura, Y. Asano, Y. Maruyama, T. Yokoyama, M. Nomura, S. Ogawa and K. Nakanishi, *J. Pharm. Sci.*, 2008, **97**, 1301; (*c*) H. Pu, Q. Liu, L. Qiao and Z. Yang, *Polym. Eng. Sci.*, 2005, **45**, 1395; (*d*) S. G. Kazarian and G. G. Martirosyan, *Int. J. Pharm.*, 2002, **232**, 81.

